Geosciences Journal
Vol. 18, No. 4, p. 427 − 437, December 2014
DOI 10.1007/s12303-014-0013-y

The evolution of permeability and gas composition during remote protective longwall mining and stress-relief gas drainage: a case study of the underground Haishiwan Coal Mine

Wei Li — *Faculty of Safety Engineering, China University of Mining & Technology, Xuzhou 221116, China*; *National Engineering Research Center for Coal & Gas Control, China University of Mining & Technology, Xuzhou 221116, China*; *The Key Laboratory of Coal-based CO_2 Capture and Geological Storage, China University of Mining & Technology, Xuzhou 221116, China*

Yuan-ping Cheng*, Pin-kun Guo, Feng-hua An, Ming-yi Chen — *Faculty of Safety Engineering, China University of Mining & Technology, Xuzhou 221116, China*; *National Engineering Research Center for Coal & Gas Control, China University of Mining & Technology, Xuzhou 221116, China*

ABSTRACT: The mining of protective coal seams can cause changes in geostress, leading to changes in the permeability of coal rock and creating favorable conditions for gas extraction from coal seams. At the Haishiwan Coal Mine, field tests using remote protective coal seam mining were performed in the protected layer, which is rich in CO_2 gas. In remote protective longwall mining, the permeability and composition of extracted stress-relief gas can vary. Under the conditions of remote protective longwall mining, the permeability of a protected coal seam can be generally described by the Liu model. During protective layer mining, the permeability of the protective layer increases rapidly with the release of stress, then decreases gradually with the recovery of the geostress. However, matrix shrinkage and decreased pore pressure caused by CO_2 desorption from coal seams also cannot be ignored when considering the factors that affect the permeability. Thus, it is necessary to appropriately configure the cross-measure boreholes in advance to drain the stress-relief gas during remote protective layer mining. Stress-relief CO_2 gas extraction presents multiple consecutive peaks. The No. 2 coal seam has different trap pressure systems as CO_2 migrates into the coal seam. The protected seam experiences different effective stresses during protective layer mining, and the permeabilities appear to periodically increase due to differences in the original permeability. The various permeability and diffusion coefficients for CO_2 and CH_4 in coal induce CO_2 and CH_4 fractionation in the roof and floor of the No. 2 coal seam.

Key words: permeability, gas component, remote protective longwall, stress-relief

1. INTRODUCTION

Driven by robust economic development, China has become the world's second largest energy producer and consumer. Coal, as a primary energy source, accounts for 70% of the nation's total energy supply. Chinese coal production increased significantly from 1299 million metric tons (Mt) in the year 2000 to 3500 Mt in 2011, an annual growth rate of 10% (BP, 2010). It is predicted that coal will continue to play a leading role in the energy structure of China for many years. The depth of coal mining has increased at a rate of 30–50 m/year in China. As coal mining depths have increased, accompanying increases in geostress and coal seam gas pressure and content have been observed. However, the permeability of coal seams appears to decrease with depth, which has contributed to a growing number of coal and gas outburst and gas explosion disasters (Wang et al., 2012). Mining of the upper protective coal seam is preferred in coal seam groups, according to the provisions of the "Prevention of Coal and Gas Outbursts Law" (State Administration of Work Safety, 2009). Although it poses a major threat to coal mine safety, methane is also a clean and high-efficiency fuel (Flores, 1998). The energy released in the combustion of 1 m^3 of methane at standard temperature and pressure is 35.9 million Joules, equivalent to the combustion of 1.2 kg of standard coal. At the same time, methane is also an intense greenhouse gas with 25 times the environmental impact of carbon dioxide (a factor known as the Global Warming Potential, or GWP). By encouraging methane drainage through increased use of coal mine methane, the Chinese government expects to promote mining safety and reduce greenhouse methane emissions for sustainable development of coal mining (Cheng et al., 2011).

A protective seam is one that can be mined without gas outburst, such that the burst-prone coalbed can be over- or under-mined (Braüner, 1994). Under coal seam group conditions, no- or low-outburst danger coal seams are identified as protective coal seams, and the protected seams are then defined in relation to them (within the zone influenced by

*Corresponding author: ypchengcumt@126.com; weilcumt@hotmail.com

mining activities). Protective coal seam mining relieves geologic stresses and increases deformation of the adjacent coal or rock layer; as a result, the permeability of the coalbed or rock will increase significantly through the formation of cracks and bed-parallel fractures (Chen et al., 2013). Methane in both protective and protected coal seams may subsequently flow into the protective coal face through low stress, high permeability regions (Noack, 1998; Díaz Aguado and González Nicieza, 2007; Wang et al., 2013). Protective coal seams are categorized as either "upper" or "lower" based upon the stratigraphic relationships of the coalbeds. Strata movement, hydraulic head changes, and gas emissions after the mining of lower protective coal seams have been extensively studied (Zhang et al., 2007; Sang et al., 2010; Yang et al., 2011a; Schatzel et al., 2012), however, research on coal seam floor deformation after mining of upper protective seams is limited. Fracturing and deformation of upper longwalls caused by mining is associated with expansion of underlying strata (such as coal seams) and creates a system of fluid pathways in lower coal seams that greatly affect permeability and gas migration. This study analyzes the geomechanical phenomena and stress-relief gas drainage of the lower protected coal seams in the Haishiwan mine that result from mining of the upper protective coal seam.

High concentrations of CO_2 have been observed in the coal of the No. 2 seam (a protected seam) and in the ambient air of the coal mine (Li et al., 2011). The CO_2-saturated coal seam is characterized by high pressure, high ground temperature and low permeability at a mining depth of 700–800 m (Li et al., 2013). CO_2 has more than twice the affinity for coal than does CH_4; the CO_2 injected during the mining process displaces coalbed CH_4, and significant coal swelling due to CO_2 saturation has been observed in a range of coal samples in laboratory experiments (Karacan, 2003). In the present study, changes in permeability and gas composition during remote protective longwall mining and stress-relief gas drainage were recorded and analyzed under in situ coal seam conditions.

2. GEOLOGIC SETTING

The Yaojie coalfield is located on the western margin of the Minhe Basin and extends across Gansu and Qinghai provinces. The Proterozoic basement is composed of marble, gneiss, quartz schist, and siliceous limestone, making up a cluster of metamorphic rocks with a thickness greater than 6000 m that outcrop near the Yaojie coalfield (Wei et al., 2007). The coal-bearing strata of the Yaojie coalfield are part of the Middle Jurassic Yaojie Series. The Yaojie coalfield extends in a roughly NNW direction, with a major fault zone known as "F19" forming the eastern boundary of the Yaojie. The F19 fault is normal to both the Cretaceous strata exposed in the hanging wall and the Jurassic strata exposed in the footwall. The fault trends in a N-S direction and ends oriented to the east. The coal basin rests stratigraphically atop the Huangyuan Group.

The Haishiwan coal deposits are located in the deepest part of the Yaojie coalfield, consisting of the Haishiwan and Jinhe Coal Mines (Fig. 1). These seams are primarily located in the Jurassic Yaojie Group; two of the three coal seams are suitable for mining. The No. 1 coal seam is comprised of sapropelic coal that is free of gas outbursts, and its upper portion averages 4 m in thickness. The No. 2 coal seam is particularly suitable for mining, although it presents a significant hazard of CO_2 outbursts. The thickness of the No. 2 coal seam ranges from 19 to 50 m with gradual thinning from the west to the east of the coalfield. The regional geological evolution, geological structure and stratigraphy of the Haishiwan coalfield were described in detail by Li et al. (2011). In the Haishiwan region, the No. 1 and No. 2 coal seams are considered the remote protective and protected seams, respectively. The vertical spacing between the No. 1 and No. 2 seams is 27–55 m, and the maximum vertical spacing is 90 m relative to the thickness of the No. 2 seam. Mining of the upper zone of the No. 1 coal seam induced changes in the strata stresses, fractures, and gas flow of the lower No. 2 coal seam. Thus, it is necessary to conduct drilling to drain the gas in these high-permeability regions to eliminate the outburst hazard of the No. 2 seam.

3. STRESS EVOLUTION OF THE UNDERLYING ROCK AND COAL SEAM DURING LONGWALL MINING

It has been proposed that under the combined effects of gravitation and hydraulic pressure, the rock mass is subjected to a distributed compression in front of the mining face, horizontal compression in the upper floor layer and horizontal extension in the lower layers of the floor strata. In this way the initial cracks or joints in strata of the lower floor generate additional tensile fractures within the rock. The rock mass of the upper floor is in a transitory state of compression and releases excess elastic energy, resulting in brittle fracture (Wang and Park, 2003).

The maximum depth of a fracture is dependent on the width of the plastic zone near the mining face as well as the frictional angle of the strata of the floor. By employing the plastic slip-line theory for calculating load on an infinite continuum, the maximum depth (h_1) of a fracture in the floor strata can be derived as follows (Zhang et al., 1997):

$$h_1 = \frac{x_a \cos\varphi_0}{2\cos\left(\frac{\pi}{4}+\frac{\varphi_0}{2}\right)} \exp\left[\left(\frac{\pi}{4}+\frac{\varphi_0}{2}\right)\tan\varphi_0\right], \quad (1)$$

where x_a is the width of the plastic zone of the coal seam near the mining face, and φ_0 is the internal frictional angle of the floor strata. The maximum depth of a fracture is not more than approximately 25 m according to Equation (1). This result agrees with estimates of conditions in the Haishiwan Coal Mine, notably that the No. 2 coal seam is located in

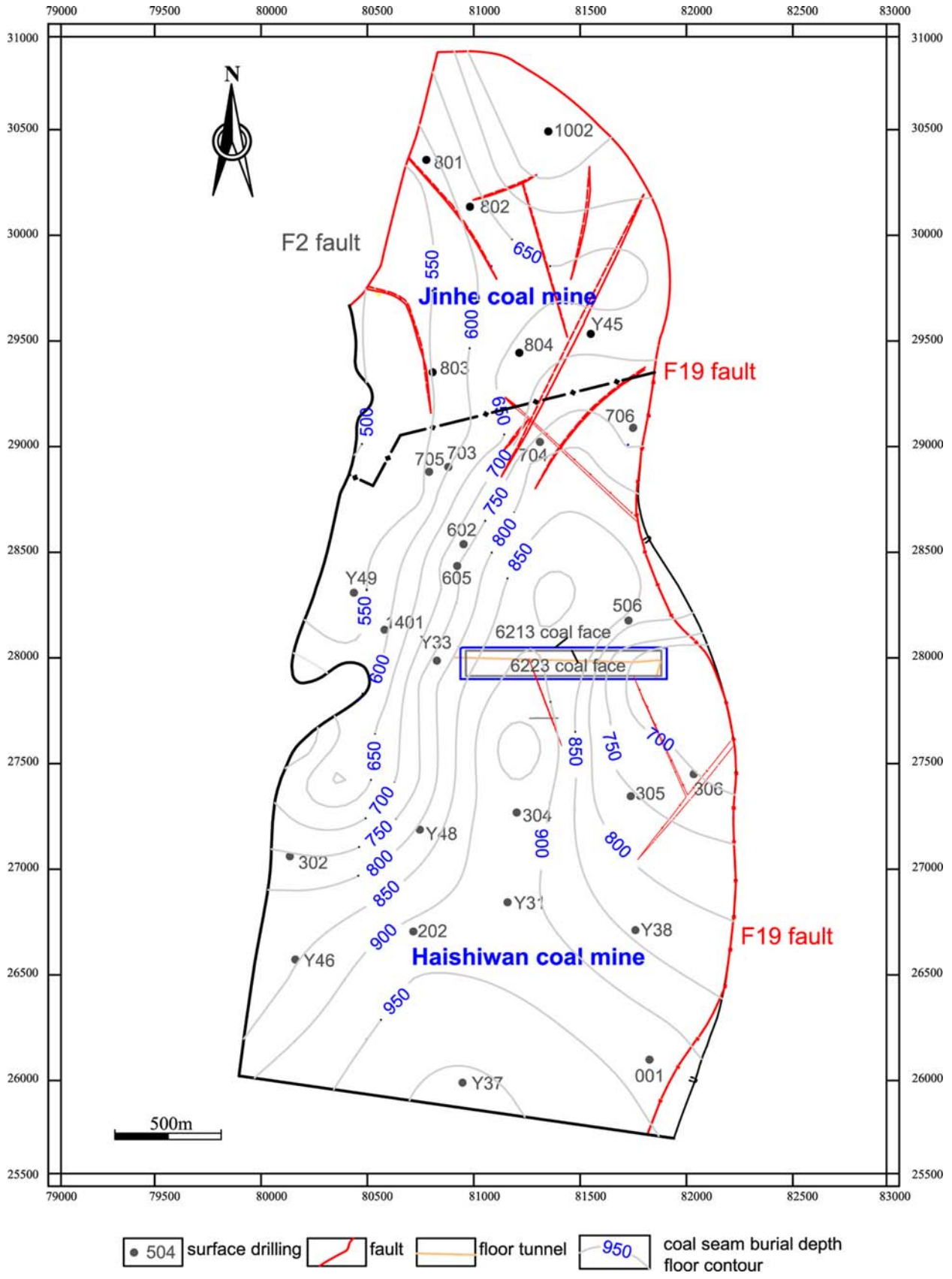

Fig. 1. The floor depth contour map for the No. 2 coal seam in the Haishiwan coalfields, and the arrangement of the exploration boreholes and coal face.

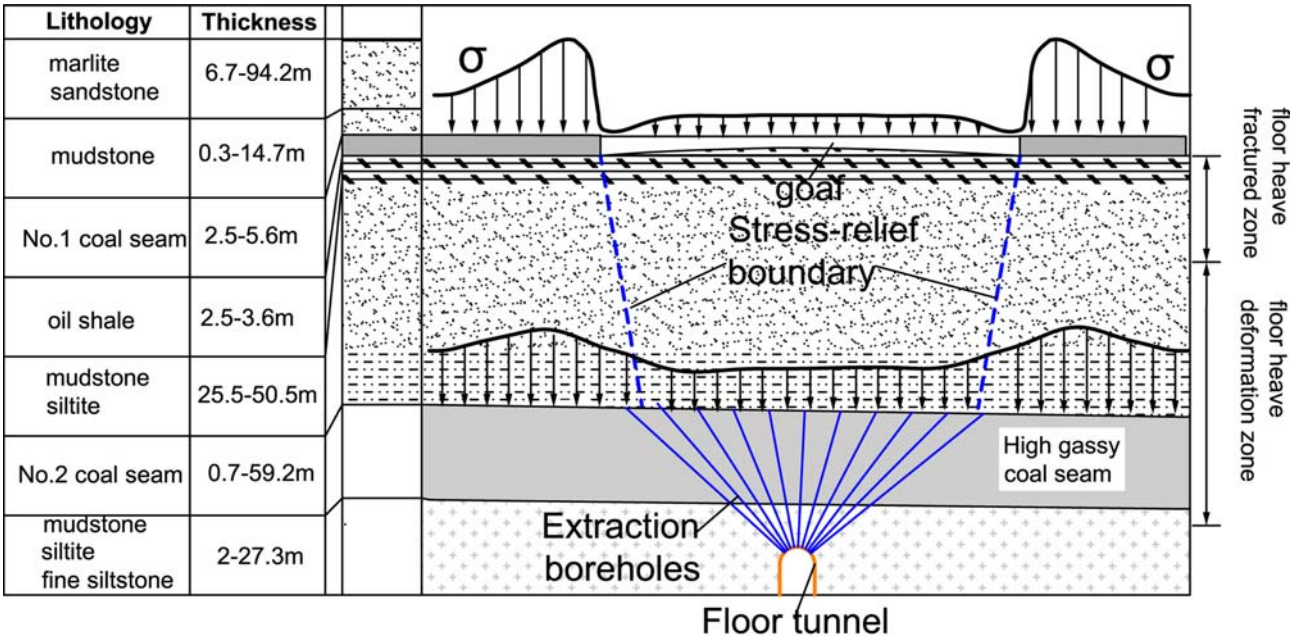

Fig. 2. The in situ stress distribution of the protective seam (No. 1 coal seam) and protected seam (No. 2 coal seam) during protective seam mining in the Haishiwan coalfield formation.

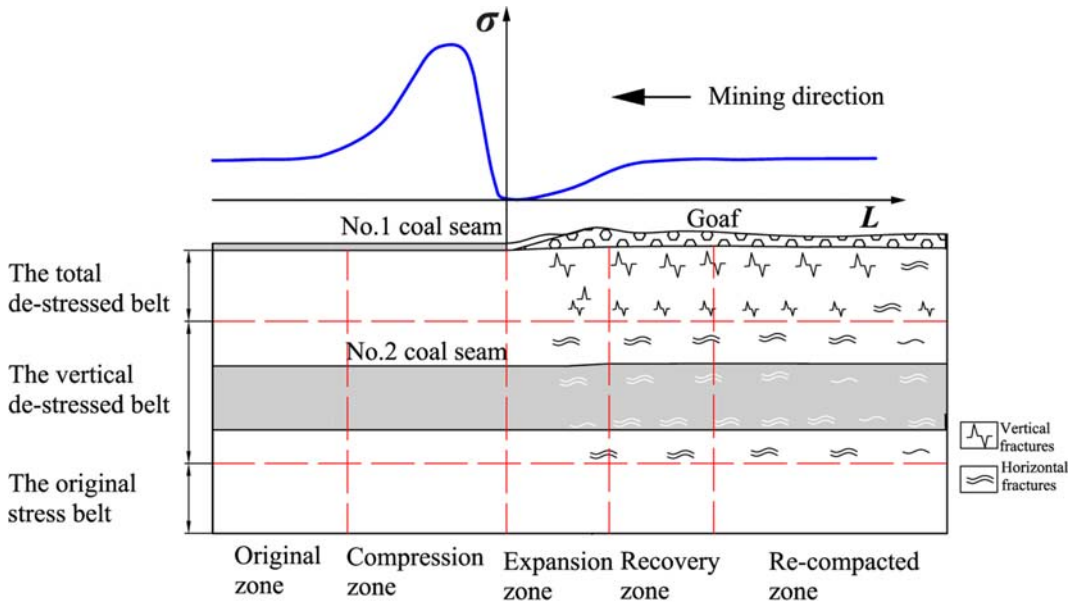

Fig. 3. Comparison of stress and displacement of the rock mass below the protective seam along the mining direction.

the elastic deformation zone of the mine floor (Fig. 2).

The rock mass below a protective coal seam can be divided into several zones in the vertical and horizontal directions based on the distribution of stresses and differences in displacement. The following zones occur along the mining axis: original zone, compression zone, expansion zone, recovery zone and re-compacted zone. Three zones occur perpendicular to the mining axis according to the stress state: the total de-stressed belt, the vertical de-stressed belt and the original stress belt. When the protected coal seam is located in the expansion zone and stress-relief belt, each of these zones has different values for the mining rate, mining depth and pore pressure, determined by the lithology of the zones (Fig. 3). The change in the stress state causes damage to the coal seam, increasing its permeability. The stress-relief belt is shaped like an inverted trapezoid located between the protective and protected coal seams, and is based on propagation of the mining stresses (Yang et al., 2011). Many field tests and numerical analyses have yielded similar relationships (Zhao et al., 2000; Yang et al., 2011b).

4. PROTECTED COAL SEAM PERMEABILITY AS PREDICTED BY EVOLUTION THEORY

High concentrations of CO_2 have been observed in the No. 2 coal seam in the Haishiwan coalfield. The eastern area has a CO_2 content of greater than 90%, whereas in the western area the CO_2 content is estimated to be less than 50%. The measured gas pressure values range from 1.0 MPa to 7.5 MPa. The CO_2-CH_4 content distribution law of the coal seam partial CO_2 pressure is different from that of the coal seam CH_4 pressure.

Owing to the dual-porosity structure of coal seams (Lu and Connell, 2007), the coal matrix represents the main reservoir for the gas, and the cleats are the main fracture pathways. The net change in permeability that accompanies gas production is thus controlled by the competing effects of declining pore pressure acting to decrease permeability, and the shrinking coal matrix acting to increase it (Zhang et al., 2008). During production or enhanced coalbed methane recovery, the pore pressure and gas content change. Pore pressure changes lead to compressibility responses from the solid and pore structure of the coal. At the same time, gas content changes lead to strain on the coal matrix. Many models that include the impact of effective stress and coal swelling/shrinkage have been developed to describe coal permeability. In the case of CO_2, significant swelling or volume increases were observed for a range of coal samples in laboratory experiments (Karacan, 2003; Pan and Connell, 2007; Pini et al., 2009), so coal permeability models must account for the effects of stress as well as coal swelling or shrinkage. The stress-controlled permeability model has been used to study permeability change relationships under remote longwall mining, as reported by Liu et al. (2011). The resulting permeability expressions for both the matrix and fracture systems of a coal seam can be expressed as follows:

$$\frac{k}{k_0}=\frac{k_{m0}}{k_{m0}+k_{f0}}\left(1+\frac{\alpha}{\phi_{m0}}R_m\frac{\Delta\sigma-\Delta p_m}{K}\right)^3+\frac{k_{f0}}{k_{m0}+k_{f0}}\left[1+\frac{(1-R_m)}{\phi_{f0}}\left(\frac{\Delta\sigma-\Delta p_f}{K}-\frac{\varepsilon_L p_L}{p_L+\Delta p}\right)\right], \quad (2)$$

where K is the bulk modulus of the coal-fracture assemblage; α is Biot's coefficient; $\Delta\sigma$ is the stress difference; Δp_m, Δp_f are the pore pressure differences of the coal matrix and fracture, respectively; φ_{m0}, φ_{f0} are the initial porosities of the coal matrix and fracture, respectively; k_{m0}, k_{f0} are the initial permeability values of the coal matrix and fracture, respectively; R_m is the modulus reduction ratio, ranging between 0 and 1; ε_L the sorption-induced strain constant, represents the volumetric strain at infinite pore pressure with the Langmuir pressure constant, p_L, which represents the pore pressure at which the measured sorption-induced strain is equal to 0.5 ε_L.

Stresses within underlying coal and rock strata decrease subsequent to protective coal seam mining. This change in stresses is closely related to the interlayer spacing, mining thickness, lithology and other factors. The rock mass below the protective coal seam can be divided according to the stress state into the total de-stressed belt, the vertical de-stressed belt and the original stress belt (Yang et al., 2011a). The rock mass stress changes in a dynamic manner, leading to spatial and temporal variations in permeability. This stress-sensitive permeability increases significantly under longwall mining as a result of stress relief, after which the longwall goaf stress recovery leads to a gradual decrease in the permeability (Fig. 4). The resulting permeability increase causes the adsorbed gas to desorb and flow freely within the crack network. The shrinking and the decrease in effective stress of the coal matrix further increase permeability. The magnitude of the permeability increase is likely limited only by the magnitude of the pressure decrease (Fig. 4a). Under the Haishiwan Coal Mine's conditions, the maximum depth of a fracture is no more than 25 m. As the fractures expand in all directions up to that 25 m limit, they connect with one another to form the perfect desorbed-gas flow network, and the desorbed gas

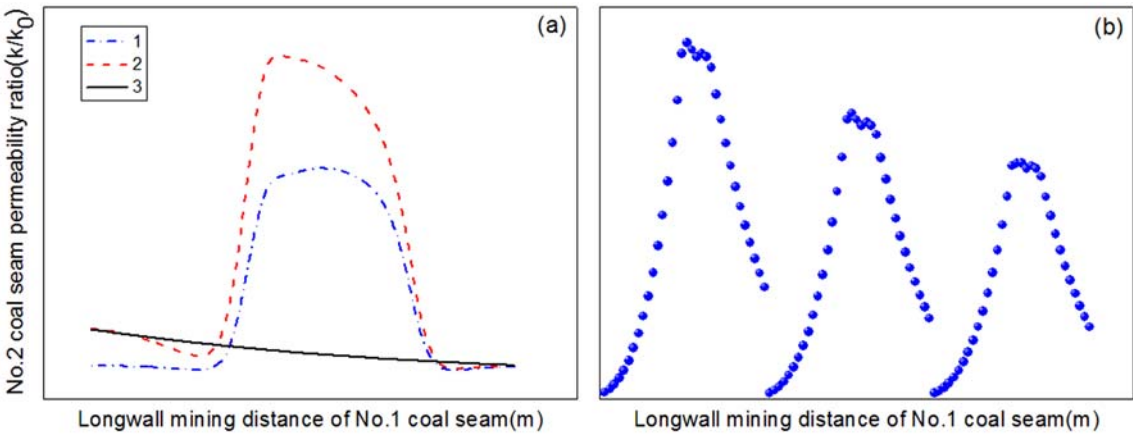

Fig. 4. The evolution of the permeability of the No. 2 coal seam during No. 1 coal longwall mining at different effective stresses. (a) The geostress and pore pressure decrease differently; (b) No. 2 coal seam shows different pore pressures in the mining direction.

can flow through the No. 2 coal seam – yet cannot flow far enough vertically to escape. Therefore, artificial diversion channels (boreholes) must be introduced to extract the gas to enhance permeability and eliminate the danger of outburst. When considering the pore pressure distribution in the Haishiwan Coal Mine, evolution of the permeability is controlled by the original pore pressure imbalance and stage mining according to the model created by Liu (2011). Cyclic variations in permeability may occur when protective coal seam mining enters an area of discontinuous coal seam pore pressure, as shown in Figure 4b.

Upper protective mining may generate stress relief in low-permeability protected seams, and the adsorbed gas will desorb and flow into the fracture network as the effective stress decreases and new coal fracture system growth occurs. However, the desorbed gas cannot flow out of the stress-relief coal seam independently because the space between protective and protected seams is large, and the mining flow channels cannot form. An artificial diversion channel should be constructed ahead of upper protective seam mining such that the desorbed gas can flow freely out of the protected seam through the artificial diversion channel (the cross-measure borehole) during the stress-relief period.

5. FIELD STUDY IN THE HAISHIWAN COAL MINE

A field study was carried out in protective longwall face 6213 and protected longwall face 6223 for the drainage of desorbed gas and elimination of outburst risk. The basic parameters of the two longwall coal faces are shown in Table 1.

The construction of the floor tunnel and cross-measure boreholes was completed prior to gas extraction. Next, the gas-extraction system was established, composed of an extraction pump station, an extraction pipeline, a gas storage tank and extraction boreholes. With these measures in place, mining of protective longwall 6213 proceeded, and the stress-relief gas flowed freely from extraction boreholes to extraction pipeline.

The floor tunnel is located in the No. 2 coal seam floor at a depth of 20 m, and the cross-measure boreholes were drilled through the full thickness of the No. 2 seam such that they penetrated more than 0.5 m into the floor tunnel. The spacing of adjacent holes and rows was 15 m × 15 m in width and length. The horizontal and vertical cross-sectional views of the two longwall faces are shown in Figure 5. Each borehole was attached to a gas drainage system immediately after drill-

Table 1. The parameters of the 6213 protective longwall face and 6223 protected longwall face

Coal seam	Coal face	Mining thickness (m)	Coal seam inclination (°)	Gas content (m^3/t)	Gas pressure (MPa)	Outburst risk
No. 1	6213 Protective longwall face	3.0	4–6	2–3	None	No
No. 2	6223 Protected longwall face	2050	4–6	44.7	1.0–7.5	Yes

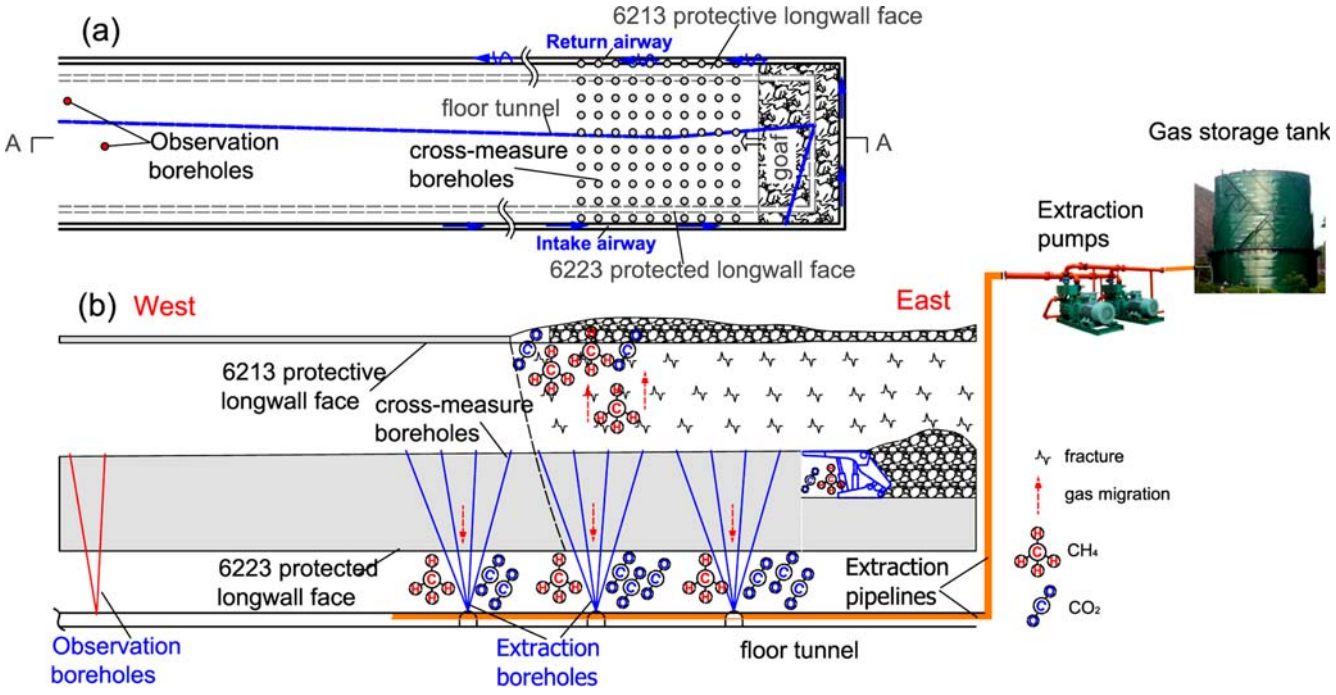

Fig. 5. Diagram of the spatial configuration of the protective longwall, protected longwall and stress-relief gas drainage. (a) Horizontal plane view; (b) vertical section view.

ing, and the gas flow rate and gas concentrations were monitored over time.

5.1. In Situ Permeability of No. 2 Coal Seam

The upper protective longwall has been in operation since February 10th, 2009. Two observation boreholes were installed in the No. 2 coal seam with a crossover distance of 70 m (Fig. 5). The gas flow rate was recorded during the mining of protective longwall 6213. The initial flow rates were 0.057 and 0.092 m^3/min for the No. 1 and 2 boreholes, respectively. The flow rate increased gradually with the distance between the boreholes and the No. 1 coal face at 40 m; in contrast, flow increased rapidly when the distance was 10 m. The vertical stress at the No. 1 coal mining face increased rapidly with distance from the face due to the mining-induced stress abutment; peak stress occurred in the No. 2 coal seam due to stress transfer over space and time. During loading, permeability began to increase, which can be explained by the competing processes of axial crack opening and oblique and transverse crack closure (Wang et al., 2013).

There was an initial increase in gas flow rate, reaching a maximum of 2 m^3/min at the coal face across the No. 1 and 2 boreholes, each 20 m distant. The data show that as soon as the strata were disturbed by mining activities, the flow rate at the boreholes fell to 0.8 m^3/min when the coal face was 35 m distant (Fig. 6).

The initial gas pressure was 3.6 MPa, and the gas pressure decreased 30 m ahead of the mining face (Fig. 6). The gas pressure suggests that mining-induced disturbances and stress relief caused coal (rock) bed swelling, with the fracture network occurring 30 m ahead of the mining face. The gas pressure decreased significantly due to the boreholes intercepting the fracture network and draining the stress-relief gases; the gas pressure decreased to zero until the mining face had passed the borehole location at 40 m (Fig. 6). In addition, the fracture network of single boreholes did not form enough channels for sufficient gas flow; the maximum gas flow rates decreased rapidly and likely continued to for some time, suggesting that the communication between these stress-relief fracture was poorly developed.

In naturally fractured formations such as coal, the permeability is sensitive to changes in stress or pore pressure. The in situ permeability of the No. 2 coal seam ranges from 0.00039 to 0.00051 mD and increases gradually due to the unloading of vertical stress. The actual maximum value is 0.042 mD, measured over 45 days in an underground coal mine (Fig. 7), which increased to approximately 100 times the in situ permeability. Under stress-controlled conditions, the in situ permeability increases due to CO_2 desorption-induced coal shrinking. Effective stress had the greatest influence on the relative permeability of CO_2 while the second greatest contributor to the final fracture permeability levels in the No. 2 coal seam was coal matrix shrinkage caused by gas desorption.

The 450 cross-measure boreholes were constructed in advance of mining the No.1 coal seam. The gas drainage volume was 0.03 million m^3/day for the first few days; at the time, the No.2 seam exhibited no stress anomalies due to mining of the No. 1 seam. After several days, the gas drainage volume increased quickly due to increasing permeability, and gas production data showed a maximum recorded value of 0.21 million m^3/day. These results demonstrate that the stress decreased and permeability increased at the No. 2 coal seam during the mining of the No.1 coal face. Coal permeability exhibited the impact of both effective stress and coal swelling/shrinkage. Permeability further increased along with gas desorption and coal matrix shrinking, and the effective stress decrease led to increased permeability, as indicated by Equation (2).

The gas drainage volume decreased over time, generally

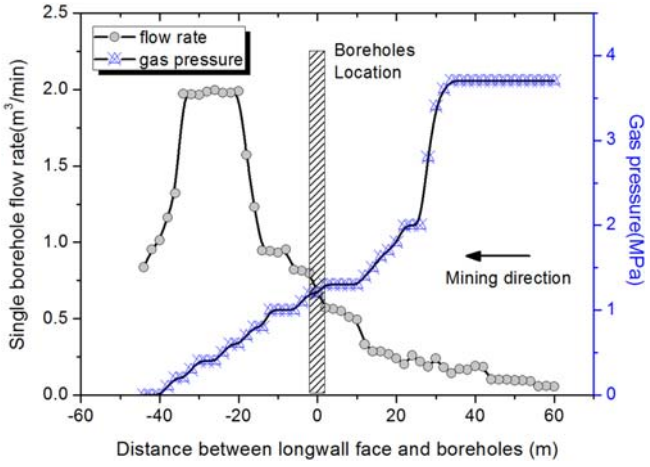

Fig. 6. The relationship between the flow rate and pressure of the relief boreholes in the lower protected layer and the mining distance of protective layer.

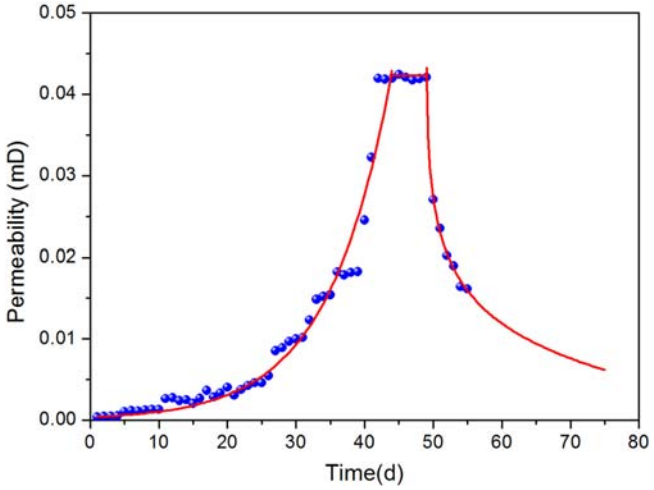

Fig. 7. Evolution of the permeability of the No. 2 coal seam with stress relief. The results are calculated for the borehole dates.

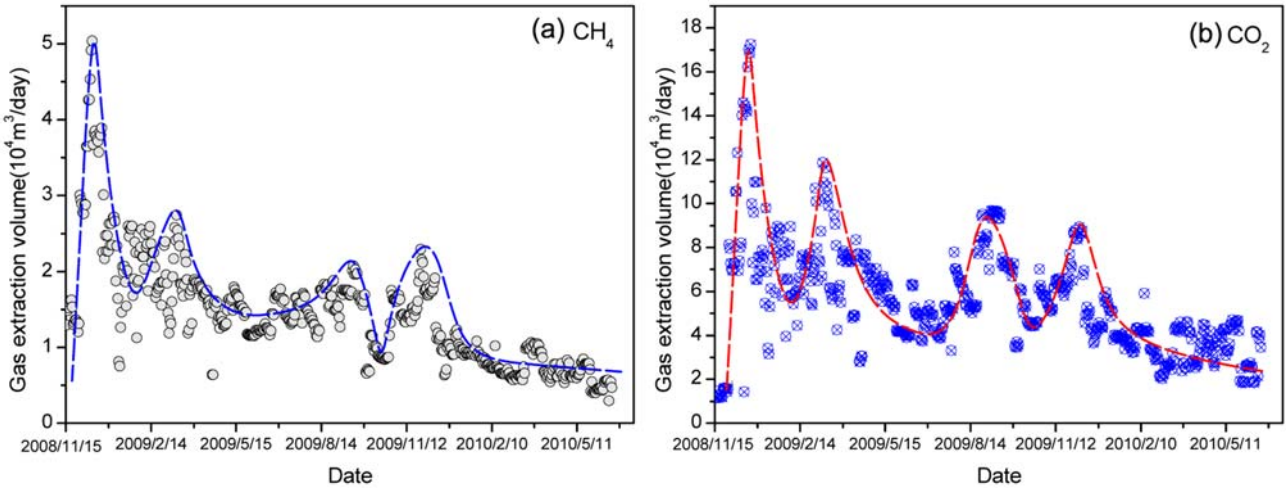

Fig. 8. Evolution of the stress-relief drainage gas in the floor tunnel over time. (a) Methane; (b) carbon dioxide.

increasing in a power function relationship. The rock mass below the protective coal seam can be divided into different stress states in the vertical and horizontal directions, following a cyclical pattern in space and time. During the mining process, the rock mass stress in the different belts changes dynamically and causes permeability differences within the same belt (Yang et al., 2011a). The high pore pressure of the No. 2 coal seam results in an effective stress decrease during the No. 2 coal seam unloading process, and the unloading of tensile stress causes the overlying rocks to swell and damage easily. In addition, a numerical study of the fracture behavior of the floor strata showed that a higher coal seam pressure corresponds to the deepening and growth of fractures (Wang and Park, 2003).

However, the variation curve of the CO_2 drainage volume over time is different from that of CH_4 (Fig. 8a). Four apparent peak values were observed on the CO_2 drainage volume curve; a similar four-peak pattern emerged on the CH_4 drainage volume curve (Fig. 8b). Previous studies observed inorganic CO_2 migration into the No. 2 coal seam through the F19 fault, located on the eastern boundary of the coalfield. This eastern area has a CO_2 content greater than 90%, whereas in the western area the CO_2 content is estimated to be less than 50% (Li et al., 2011; Li et al., 2013). The CO_2 content decreases and the CH_4 content increases with distance from the F19 fault. The CO_2 content of the reservoir gas leaking through F19 fault into the coal seams is related to changes in this imbalance, and is stable over long periods of geologic time. The measured gas pressure values range from 1.0 MPa to 7.5 MPa, decreasing linearly with distance from the F19 fault. The No. 2 coal seam has various trap systems along the F19 fault. As shown in Figure 9, the gas pressure is expressed by $p_1 > p_2 > p_3 > p_4$ (Li et al., 2013), which was also demonstrated during enhanced coalbed methane recovery with CO_2 injection (Shi et al., 2008). Low-permeability zones occur within the different gas pressure systems, hindering

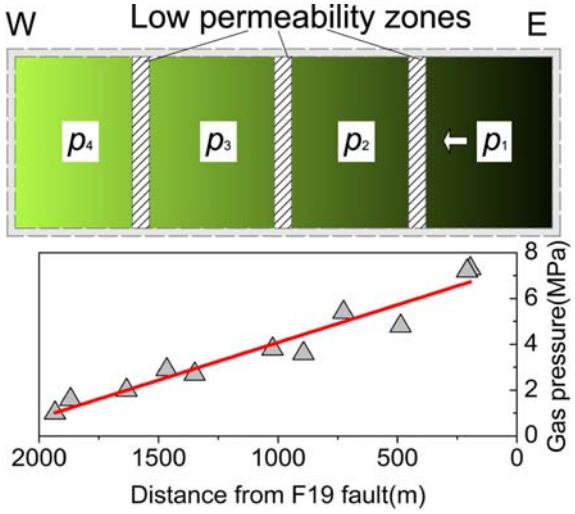

Fig. 9. Variation in the gas pressure in the protected coal seam (6223 coal longwall) based on gas pressure tests in the underground Haishiwan Coal Mine. The gas pressure decreases gradually from east to west.

development of gas pressure balance in the No. 2 coal seam over geologic time scales. The same original stress and the different pore pressures together suggest different effective stresses and different initial permeability before protective layer mining, and the protected seam experiences different effective stresses during protective layer mining. The different effective stresses in fact determine the initial permeability, so the permeability appears to increase periodically due to differences in the initial permeability under the same stress-relief conditions. The gas content decreases with distance from the F19 fault, and thus, the stress-relief gas accordingly presents periodic changes. The increase in permeability as the coal matrix shrinks after gas desorption also cannot be neglected.

Many studies have described the penetration of CO_2 in coal with evidence that the macromolecular structure changes

during the sorption process involving the glassy and elastic structure of coal (Larsen, 2004; Goodman et al., 2006). CO_2 diffuses into the polymeric network of the coal material; the swelling of coal due to a penetrant can be referred to as an increase in the volume occupied by the coal. Although the rearrangement is largely controlled by the coal, the effect of the CO_2 as a plasticizer increases the free volume, thus lowering the glass-transition temperature (T_g) and enabling the rearrangement. (Karacan, 2003; Mirzaeian and Hall, 2006). CO_2 desorption and flow out of the coal matrix leads to an increase in T_g; conversely, the CO_2 diffusion coefficient decreases as the coal matrix shrinks after CO_2 desorption at low pressure. High-pressure CO_2-saturated coal can easily enter an elastic state with a lower glass transition temperature, and the CO_2 diffusion coefficient in the elastic state is higher than that in the glass state of coal (Govindjee and Simo, 1993; Mazumder et al., 2011). CO_2 can diffuse faster through coal matrix than CH_4 during stress-relief gas drainage, therefore the maximum CO_2 drainage volume is greater than that of CH_4.

5.2. Gas Composition Evolution during Mining

During the extraction of coalbed gas in the Haishiwan Coal Mine, the ratio of CO_2 to CH_4 of the gas mixture was obtained by extraction based on regular monitoring of the gas concentration and extraction quantity in the main extraction pipeline, as shown in Figure 10a. The ratios of CO_2/CH_4 range from 2.33 to 6.00, with an average of 3.93. With increasing extraction time, the ratio of CO_2/CH_4 increases. The extraction boreholes drainage area is fixed, and during extraction, the proportion of CO_2 gradually increases (i.e., after the pressure relief of the coal seam, CH_4 desorbs and diffuses prior to CO_2). As the extraction time increases, the CH_4 desorption capacity is gradually reduced, and the relative desorption capacity of CO_2 increases.

Fresh air from the mine's ventilation system flows from the intake airway and through the coal face, where it dilutes the seam gas concentrations; then the ventilation air and seam gas flow back out of the coal face through the return airway. The ratio of CO_2 to CH_4 in ventilation air gas is obtained by gas concentration monitoring (Fig. 5a). The ratio of CO_2/CH_4 in the ventilation discharge of the 6213 working face first increases and then decreases during work-face removal (Fig. 10b). Over the several months during which the 6213 face was mined, the ratios of CO_2/CH_4 increased rapidly to values between 2.5 and 4.0. During work-face removal, the ratios gradually decreased linearly, with values ranging from 1.5 to 2.05. The heterogeneous pore structure of coal seams has been closely approximated by a dual-porosity model, which assumes that Darcy flow occurs in the cleat system, whereas gas diffusion is the dominant process in the coal matrix (Bush et al., 2004). During ventilation gas production, the desorbed gases from the internal pores diffuse through the coal matrix to reach the cleat system and then flow to the production well. The adsorption, diffusion and flow of gas in the coalbed play important roles in gas production.

Many experiments have shown that CO_2 is preferentially adsorbed from an equimolar $CO_2 + CH_4$ mixture (Busch et al., 2003). Accordingly, component adsorption isotherms demonstrate that methane is preferentially released at higher pressures during desorption (Busch et al., 2003). Gas desorption occurs when the stress decreases and the coal matrix expands, and the previously desorbed CH_4 flows into extraction boreholes under a negative-pressure environment. Remote protective longwall mining could not form an abundance of macrofractures within the No. 2 coal seam. However, many macropores arose due to the stress relief as well as desorp-

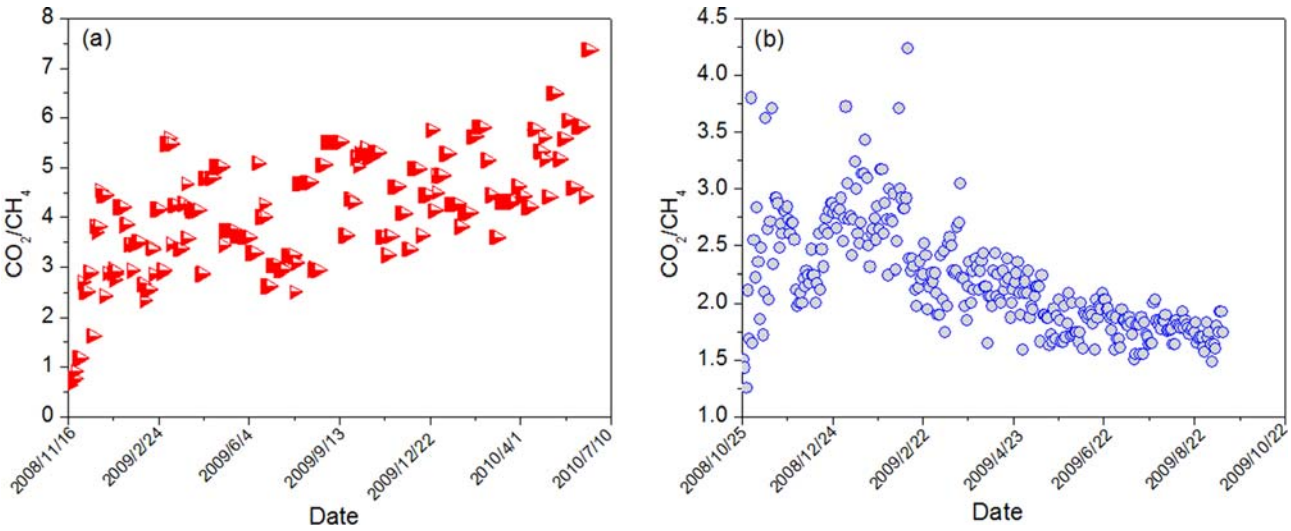

Fig. 10. (a) Variations in the drainage CO_2/CH_4 values in the floor over time; (b) changes in the ventilation air CO_2/CH_4 values with distance from the 6213 working face.

tion and matrix shrinkage, and gas diffusion was the main mechanism of mass transfer in the coal seam.

Due to its relatively small kinetic diameter, CO_2 can permeate not only macropores but also ultra-micropores which likely block CH_4, it having a slightly larger kinetic diameter. This effect results in a diffusivity of CO_2 that is one or two orders of magnitude higher than that of CH_4 in the coal matrix (Cui et al., 2004). The pore pressure of the No. 2 coal seam decreases during gas drainage, and the permeability of the No. 2 coal seam decreases due to overburden stress recovery. However, the diffusivity of CO_2 in the coal matrix increases significantly with decreasing gas pressure, which leads to increasing CO_2/CH_4 values in the drainage gas over time.

The CO_2/CH_4 value of the 6213 coal face ventilation discharge reflects the gas emission of the coal face seam floor. Under both gas pressure and mining-induced pressure, the floor strata failed to indicate that the fractures were connected to the No. 2 coal seam and mining area, and the space between the No. 1 and No. 2 coal seams became smaller in the mining direction. The unloading effect within the mined area gave rise to a higher permeability in the floor strata. The stress-relief gas of the No. 2 coal seam flowed into the 6213 coal face through the rock layers under ambient ventilation conditions. Permeability test results for sandstone and claystone rock types have shown that the permeability of both the floor and roof rocks decreases with gas pressure and that the CH_4 permeability is greater than that of CO_2 for all pressures and for both rock types (Saghafi and Pinetown, 2011). The CH_4 concentration is estimated to be greater than 50% in the 6213 longwall mining direction, and the macropore diffusivity of CH_4 and the counter-diffusivity of CH_4-CO_2 increase with an increasing CH_4 mole fraction in the gas phase. The macropore diffusivities of CH_4 are generally larger than those of CO_2 (Wei et al., 2007). The higher CH_4 permeability for rock and higher CH_4 macropore diffusivities for coal cause the CO_2/CH_4 values in the ventilation discharge of the 6213 coal face to decrease in the 6213 coal longwall mining direction.

6. CONCLUSIONS

1) The permeability of protected coal seams increases as the geostress and gas pressure of the protected layer decrease under remote protective layer mining conditions. Subsequently, the permeability decreases with the stress recovery. However, the permeability remains higher than the original permeability due to the shrinkage of the coal matrix after gas desorption, as described by Liu et al.'s model (2011). The point permeability begins to increase prior to protective layer mining due to the mining-induced stress abutment in the field. This phenomenon can be explained by the competing processes of axial crack opening, and oblique and transverse crack closure. The main purpose of cross-measure boreholes is to drain stress-relief gas during the optimal stress-relief period, so they should be constructed ahead of the upper protective seam mining.

2) There are four apparent peak values on the CO_2 drainage volume curve; these maxima are also observed in the CH_4 drainage volume curve. The protected seam experiences different effective stresses during protective layer mining, and the permeability values appear to increase periodically due to differences in the initial permeability. CO_2 diffused into the polymeric network of the coal material and caused it to swell. High-pressure CO_2-saturated coal can readily enter an elastic state with a lower glass transition temperature, and the CO_2 diffusion coefficient in the elastic state is greater than in the glass state of coal during CO_2 desorption and diffusion out of the coalbed. Thus, the maximum CO_2 drainage volumes were greater than those of CH_4.

3) With increased extraction time, the ratio of CO_2/CH_4 increased in the main extraction pipeline located in the lower 6223 coal face. However, during work-face removal, the ratio of CO_2 to CH_4 decreased during the ventilation discharge of the 6213 working face. The prior desorption of CH_4 and greater diffusivity of CO_2 in the coal matrix increased significantly with a decrease in gas pressure, leading to increasing CO_2/CH_4 values in the gas drainage. The highest CH_4 concentrations occurred at the western zone of the 6223 coal face, which showed a higher CH_4 permeability. The larger macropore diffusivity of CH_4 and greater CH_4 mole fraction in the gas phase resulted in a decrease in the CO_2/CH_4 values in the ventilation discharge of the 6213 coal face.

ACKNOWLEDGMENTS: This research was financially supported by the Natural Science Foundation for the Youth of China (No. 41202118) and the Fundamental Research Funds for the Central Universities (No. 2012QNB03) and the open fund of The Key Laboratory of Coal-based CO_2 Capture and Geological Storage, Jiangsu Province (2011KF04). A project funded by the priority academic program development of Jiangsu Higher Education Institutions.

REFERENCES

BP, 2010, BP Statistical Review of World Energy 2010, British Petroleum, plc, 45 p.

Braüner, G., 1994, Rockbursts in Coal Mines and Their Prevention. Balkema, Rotterdam, 152 p.

Busch, A., Gensterblum, Y., and Krooss, B.M., 2003, Methane and CO_2 sorption and desorption measurements on dry argonne premium coals: Pure components and mixtures. International Journal of Coal Geology, 55, 205–224.

Busch, A., Gensterblum, Y., Krooss, B.M., and Littke, R., 2004, Methane and carbon dioxide adsorption/diffusion experiments on coal: an upscaling and modelling approach. International Journal of Coal Geology, 60, 151–168.

Chen, H., Cheng, Y.P., Zhou, H., and Li, W., 2013, Damage and permeability development in coal during unloading. Rock Mechanics and Rock Engineering, 46, 1377–1390.

Cheng, Y.P., Wang, L., and Zhang, X.L., 2011, Environmental impact of coal mine methane emissions and responding strategies in China. International Journal of Greenhouse Gas Control, 5, 157–166.

Cui, X.J., Bustin, R.M., and Dipple, G., 2004, Selective transport of CO_2, CH_4 and N_2 in coals: insights from modelling of experimental gas adsorption data. Fuel, 83, 293–303.

Díaz Aguado, M.B. and González Nicieza, C., 2007, Control and prevention of gas outbursts in coal mines, Riosa-Olloniego coalfield, Spain. International Journal of Coal Geology, 69, 253–266.

Flores, R.M., 1998, Coal-bed methane: from hazard to resource. International Journal of Coal Geology, 35, 3–26.

Goodman, A.L., Favors, R.N., and John, W.L., 2006, Argonne coal structure rearrangement caused by sorption of CO_2. Energy and Fuels, 20, 2537–2543.

Guo, H., Yuan, L., Shen, B.T., Qu, Q.D., and Xue, J.H., 2012, Mining-induced strata stress changes, fractures and gas flow dynamics in multi-seam long wall mining. International Journal of Rock Mechanics and Mining Sciences, 54, 129–139.

Larsen, J.W., 2004, The effects of dissolved CO_2 on coal structure and properties. International Journal of Coal Geology, 57, 63–70.

Li, W., Cheng, Y.P., and Wang, L., 2011, The origin and formation of CO_2 gas pools in the coal seam of the Yaojie coalfield in China. International Journal of Coal Geology, 85, 227–236.

Li, W., Cheng, Y.P., Wang, L., Zhou, H.X., Wang, H.F., and Wang, L.G., 2013, Evaluating the security of geological coalbed sequestration of supercritical CO_2 reservoirs: The Haishiwan coalfield, China as a natural analogue. International Journal of Greenhouse Gas Control, 13, 102–111.

Liu, J., Chen, Z., Elsworth, D., Miao, X., and Mao, X., 2011, Evolution of coal permeability from stress-controlled to displacement-controlled swelling conditions. Fuel, 90, 2987–2997.

Lu, M. and Connell, L.D., 2007, A model for the flow of gas mixtures in adsorption dominated dual porosity reservoirs incorporating multi-component matrix diffusion: part I. Theoretical development. Journal of Petroleum Science and Engineering, 59, 17–26.

Karacan, C.O., 2003, Heterogeneous sorption and swelling in a confined and stressed coal during CO_2 injection. Energy and Fuels, 17, 1595–1608.

Mazumder, S., Vermolen, F., and Bruining, J., 2011, Analysis of a model for anomalous - diffusion behaviour of CO_2 in the macromolecular-network structure of coal. SPE Journal, 16, 856–863.

Mirzaeian, M. and Hall, P.J., 2006, The Interactions of coal with CO_2 and Its effects on coal structure. Energy and Fuels, 20, 2022–2027.

Noack, K., 1998, Control of gas emissions in underground coal mines. International Journal of Coal Geology, 35, 57–82.

Pan, Z. and Connell, L.D., 2007, A theoretical model for gas adsorption-induced coal swelling. International Journal of Coal Geology, 69, 243–252.

Pini, R., Ottiger, S., Burlini, L., Storti, G., and Mazzotti, M., 2009, Role of adsorption and swelling on the dynamics of gas injection in coal. Journal of Geophysical Research, 114, B04203.

Saghafi, A. and Pinetown, K., 2011, The role of interseam strata in the retention of CO_2 and CH_4 in a coal seam gas system. Energy Procedia, 4, 3117–3124.

Sang, S., Xu, H., Fang, L., Li, G., and Huang, H., 2010, Stress relief coalbed methane drainage by surface vertical wells in China. International Journal of Coal Geology, 82, 196–203.

Schatzel, S.J., Karacan, C.Ö., Dougherty, H., and Goodman, G.V.R., 2012, An analysis of reservoir conditions and responses in longwall panel overburden during mining and its effect on gob gas well performance. Engineering Geology, 127, 65–74.

Shi, J.Q., Durucan, S., and Fujioka, M., 2008, A reservoir simulation study of CO_2 injection and N_2 flooding at the Ishikari coalfield CO_2 storage pilot project, Japan. International Journal of Greenhouse Gas Control, 2, 47–57.

Wang, H.F., Cheng, Y.P., and Wang, L., 2012, Regional gas drainage techniques in Chinese coal mines. International Journal of Mining Science and Technology, 22, 873–878.

Wang, H., Cheng, Y., and Yuan, L., 2013, Gas outburst disasters and the mining technology of key protective seam in coal seam group in the Huainan coalfield. Natural Hazards, 67, 763–782.

Wang, S., Elsworth, D., and Liu, J., 2013, Permeability evolution during progressive deformation of intact coal and implications for instability in underground coal seams. International Journal of Rock Mechanics and Mining Sciences, 58, 34–45.

Wang, J.A. and Park, H.D., 2003, Coal mining above a confined aquifer. International Journal of Rock Mechanics and Mining Sciences, 40, 537–551.

Wei, X.R., Wang, G.X., Massarotto, P., Golding, S.D., and Rudolph, V., 2007, Numerical simulation of multicomponent gas diffusion and flow in coals for enhanced coalbed methane recovery. Chemical Engineering Science, 62, 4193–4203.

Yang, T.H., Xu, T., Liu, H.Y., Tang, C.A., Shi, B.M., and Yu, Q.X., 2011, Stress-damage-flow coupling model and its application to pressure relief coal bed methane in deep coal seam. International Journal of Coal Geology, 86, 357–366.

Yang, W., Lin, B.Q., Qu, Y.A., Z, S., Zhai, C., Jia, L.L., and Zhao, W.Q., 2011a, Mechanism of strata deformation under protective seam and its application for relieved methane control. International Journal of Coal Geology, 85, 300–306.

Yang, W., Lin, B.Q., Qu, Y.A., Li, Z.W., Zhai, C., Jia, L.L., and Zhao, W.Q., 2011b, Stress evolution with time and space during mining of a coal seam. International Journal of Rock Mechanics and Mining Sciences, 48, 1145–1152.

Zhang, H., Liu, J., and Elsworth, D., 2008, How sorption-induced matrix deformation affects gas flow in coal seams: A new FE model. International Journal of Rock Mechanics and Mining Sciences, 45, 1226–1236.

Zhang, J., Standifird, W.B., Roegiers, J.C., and Zhang, Y., 2007, Stress-dependent fluid flow and permeability in fractured media: from lab experiments to engineering applications. Rock Mechanics and Rock Engineering, 40, 3–21.

Zhang, J.C., Zhang, Y.Z., and Liu, T.Q., 1997, Fluid flow in rock-mass and water in-rush through coal seam floor. Geology Press, Beijing, 35 p.

Zhao, C., Hebblewhite, B.K., and Galvin, J.M., 2000, Analytical solutions for mining induced horizontal stress in floors of coal mining panels. Computer Methods in Applied Mechanics and Engineering, 184, 125–142.

Manuscript received September 10, 2013
Manuscript accepted March 28, 2014